Cell Reports
Resource

Expanding the Repertoire of Optogenetically Targeted Cells with an Enhanced Gene Expression System

Kenji F. Tanaka,[1,11,12,*] Ko Matsui,[2,12] Takuya Sasaki,[2] Hiromi Sano,[3] Shouta Sugio,[1] Kai Fan,[1,5] René Hen,[6] Junichi Nakai,[7] Yuchio Yanagawa,[8] Hidetoshi Hasuwa,[9] Masaru Okabe,[9] Karl Deisseroth,[10] Kazuhiro Ikenaka,[1] and Akihiro Yamanaka[4]

[1]Division of Neurobiology and Bioinformatics
[2]Division of Cerebral Structure
[3]Division of System Neurophysiology
[4]Division of Cell Signaling
National Institute for Physiological Sciences, Okazaki 444-8787, Japan
[5]Department of Anatomy, Dalian Medical University, Dalian 116044, China
[6]Departments of Neuroscience and Psychiatry, Columbia University, New York, NY 10032, USA
[7]Brain Science Institute, Saitama University, Sakura-ku, Saitama 338-8570, Japan
[8]Department of Genetic and Behavioral Neuroscience, Gunma University Graduate School of Medicine, JST CREST, Maebashi 371-8511, Japan
[9]Genome Information Research Center, Osaka University, Suita 565-0871, Japan
[10]Department of Bioengineering, Stanford University, Stanford, CA 94304, USA
[11]Department of Neuropsychiatry, School of Medicine, Keio University, Tokyo 160-8582, Japan
[12]These authors contributed equally to this work
*Correspondence: kftanaka@a8.keio.jp
http://dx.doi.org/10.1016/j.celrep.2012.06.011

SUMMARY

Optogenetics has been enthusiastically pursued in recent neuroscience research, and the causal relationship between neural activity and behavior is becoming ever more accessible. Here, we established *k*nockin-mediated *en*hanced *g*ene *e*xpression by improved tetracycline-controlled gene induction (KENGE-tet) and succeeded in generating transgenic mice expressing a highly light-sensitive channelrhodopsin-2 mutant at levels sufficient to drive the activities of multiple cell types. This method requires two lines of mice: one that controls the pattern of expression and another that determines the protein to be produced. The generation of new lines of either type readily expands the repertoire to choose from. In addition to neurons, we were able to manipulate the activity of nonexcitable glial cells in vivo. This shows that our system is applicable not only to neuroscience but also to any biomedical study that requires understanding of how the activity of a selected population of cells propagates through the intricate organic systems.

INTRODUCTION

There are two main approaches that one can take to understand how a complex biological system composed of numerous cells operates. One approach is to record the activities of as many cells as possible and compare these with the behavior of the entire system. By nature, this approach is a correlation study, and the causal relationship of the cells' activities and the behavior could only be estimated. The other approach is to actively manipulate the cells' activities and observe how such perturbation influences the system's behavior. Light-sensitive proteins have recently gained recognition because they can be used to control the cells' activities by use of light when it is expressed in cells (Nagel et al., 2003; Boyden et al., 2005). The advantage of this method is that, if the expression can be targeted, the physiological role of a selected population of cells in a complex system can be readily assessed.

The quickest way of applying this method is to use viruses, but this approach has problems in the reproducibility of expression patterns and levels. Therefore, we chose to use a transgenic approach, which allows stable expression. We also avoided the conventional transgenic approach, in which separate lines of animals for each promoter-protein combination are generated, because this approach seemed too laborious and because obtaining a line with sufficiently high expression levels would not be trivial.

We instead used a bigenic approach involving a tet-inducible promoter system (Gossen et al., 1995). We generated or received transgenic mice, each with a cell type-specific promoter driving a tetracycline-controlled transcriptional activator (tTA) expressing allele. We also generated transgenic mice with the tTA-dependent promoter (tetO) driving the expression of channelrhodopsin-2 (ChR2), a blue light-gated, nonselective, cation channel (Boyden et al., 2005; Nagel et al., 2003). Once equipped with both sets, we had only to perform crosses between mice from the two sets to obtain animals expressing ChR2 in a wide
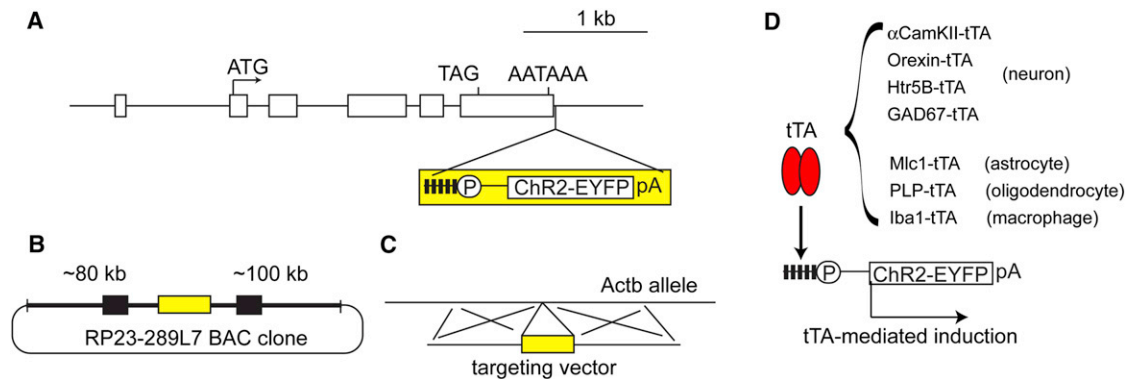
Figure 1. tetO-ChR2(C128S)-EYFP Mice

(A) Actb gene structure and insertion site of tetO-ChR2(C128S)-EYFP. The Actb gene consists of 6 exons (rectangles), and the tetO-ChR2(C128S)-EYFP polyA cassette (yellow) is inserted just downstream of the polyadenylation signal of Actb gene. AATAAA is a polyadenylation signal.

(B) BAC transgenic strategy. Modified clone RP23-289L7 contains the Actb gene followed by a tetO-ChR2(C128S)-EYFP cassette. RP23-239L7 contains the Fscn1 (filled box, left) and the Fbxl18 (filled box, right) genes.

(C) Knockin strategy. The tetO-ChR2(C128S)-EYFP cassette is inserted into the same site by homologous recombination.

(D) Cell type-specific induction of ChR2(C128S)-EYFP. tTA is expressed under the control of cell type-specific promoters. tTA transactivates the tetO promoter, and the ChR2(C128S)-EYFP fusion protein is induced in a cell type-specific manner.

See also Figure S1.

variety of selected cell populations. While ChR2 induction can be turned off by administration of doxycycline, we used the system solely to achieve cell-type specificity and amplification of transgene induction.

We previously attempted to use the tTA-mediated gene induction system to achieve specific and sufficient ChR2 expression. αCaMKII-tTA mice (Mayford et al., 1996) were crossed with mice having a bidirectional tTA-dependent promoter (bitetO) driving both ChR2-mCherry and a halorhodopsin (HaloR; a yellow light-driven chloride pump)-EGFP fusion gene that we generated (line BTR6) (Chuhma et al., 2011). The bigenic line, αCaMKII-tTA::BTR6, exhibited sparse ChR2 expression in striatal medium spiny neurons, which enabled us to conduct a connectome analysis (Chuhma et al., 2011). However, even though tTA was expressed under the control of the well-known αCaMKII promoter, the line hardly showed any ChR2 expression in the hippocampus or dorsal cortex. We have found similarly poor induction using other combinations, indicating a need for an improved system. Here we report on technical improvements that were made to overcome this limitation of the conventional tTA-mediated gene induction.

RESULTS

Improvement of the tet System

When using the tet system to achieve cell type-specific expression of ChR2, the repertoire of bigenic transgenic lines can be expanded by increasing the numbers of either the tTA or the tetO lines coding variants of ChR2. However, the tet system often fails to produce sufficient expression in the expected pattern or cellular targets. It is likely that, even with sufficient tTA being expressed, the inserted tetO promoter locus may be influenced by suppressor sequences nearby or may not be readily accessible by the increased promoter DNA methylation

or by the repressive histone modifications (Oyer et al., 2009; Zhu et al., 2007). We anticipated that knocking in the tetO-ChR2 gene at or near a housekeeping gene would lead to high levels of transactivation because: (1) we empirically noticed that the levels of tet system-mediated gene induction were extremely high when tetO was knocked into the genome by embryonic stem (ES) cell homologous recombination (Tanaka et al., 2010), and (2) the transcriptional machinery is likely to be accessible to the genome around the housekeeping gene, which may permit binding of tTA to tetO site in any cell type (Palais et al., 2009).

Based on the above reasoning and observations, we targeted transgene insertion just downstream of the β-actin gene polyadenylation signal and generated tetO-ChR2(C128S)-EYFP knockin mice by ES cell homologous recombination (knockin; Figures 1A, 1C, and S1). We chose the C128S mutant of ChR2 because it has a much higher effective sensitivity to light than does the wild-type ChR2 due to the very slow dark recovery (Berndt et al., 2009), which potentially allows stimulation of cells with even modest levels of expression. The activation/deactivation rates with blue light are slow (τ_{on} = 20 and 1.7 ms, τ_{off} = 108 s and 10 ms, for ChR2(C128S) and wild-type ChR2, respectively) (Berndt et al., 2009); however, τ_{off} can be accelerated up to 57 ms by yellow light pulse with the maximum light intensity achievable in our setup. As ChR2(C128S) allows continuous, heightened activity of the expressed cell with minimal blue light illumination, it can be used to mimic the elevated neural activity (upstate), which is often observed in in vivo recordings (Steriade et al., 1993). If the cell's action potential firing rate does not accommodate, the light-stimulated cell expressing ChR2(C128S) can potentially fire consecutively at its maximum capacity.

To determine whether the method of inserting the transgene (homologous recombination versus random insertion) has any
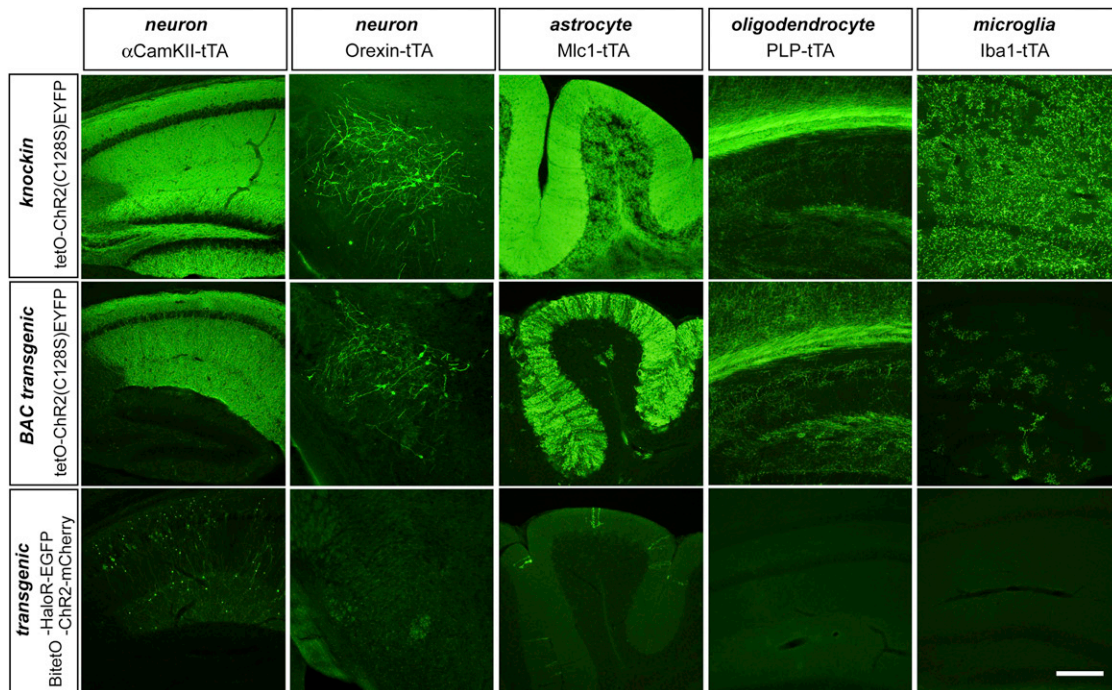
Figure 2. Superiority of the Knockin-Mediated ENhanced Gene Expression by Improved tet System over Other Transgene Expression Methods

Five cell type-specific tTA lines (columns) were crossed with three tetO lines (rows) coding light-sensitive protein (ChR2 and/or HaloR) and a fluorescent protein (EYFP or EGFP) fusion. Top, middle, and bottom row panels show EYFP immunohistochemistry of tissues from mice crossed with tetO-ChR2(C128S)-EYFP knockin mice (*knockin*), EYFP from mice crossed with tetO-ChR2(C128S)-EYFP BAC transgenic mice (*BAC transgenic*), and EGFP from mice crossed with bitetO transgenic line (BTR6; *transgenic*). tTA lines specific for neurons (αCaMKII and orexin promoter; first and second columns, respectively), astrocytes (Mlc1 promoter; third column), oligodendrocytes (PLP promoter; fourth column), and microglia (Iba1 promoter; fifth column) were used. The first, fourth, and fifth columns are from tissues of the hippocampus, the second column is from the lateral hypothalamus, and the third column is from the cerebellar lobe. Note that crossing of the cell type-specific tTA lines with tetO knockin mice (KENGE-tet system) provided the highest levels of gene expression in all cell types. Scale: 200 μm.

See also Figure S2.

effect on tTA-mediated transcription, we also generated a bacterial artificial chromosome (BAC) transgenic mouse, in which the identical cassette was inserted into the identical site downstream of the β-actin gene within the BAC (*BAC transgenic;* Figure 1B). The insertion site of the modified BAC in the mouse genome is random, but, as the tetO-ChR2(C128S)-EYFP transgene is flanked by a large fragment of genomic DNA from the site near the β-actin gene, the chromosomal positional effect, if present, is expected to be small. As a case for random insertion of the sequence starting only from the tetO promoter, we used bitetO-ChR2-mCherry and HaloR-EGFP transgenic mice (line BTR6; *transgenic;* (Chuhma et al., 2011)).

These tetO lines were crossed with cell type-specific tTA lines (Figure 1D), and the degree of tTA-mediated transcription was examined by immunohistochemistry on fluorescent proteins (Figure 2). First, the tetO lines were crossed with the αCaMKII-tTA mice (Mayford et al., 1996), in which case αCaMKII promoter activity should produce tTA expression in most pyramidal cells in the hippocampus. In the case of the tetO conventional *transgenic* mice (BTR6), tTA-mediated gene expression, as assessed by the EGFP immunohistochemistry, was sparse in the hippocampal CA1, and no expression was found in the

dentate gyrus (Figure 2, bottom). The poor expressions of HaloR-EGFP might be explained by the aggregate formation of this protein because the original version of the HaloR-EGFP that we used was often found to aggregate easily. However, we failed to detect even the mRNA of HaloR-EGFP in the dentate gyrus, indicating that tTA-mediated transactivation was limited in tetO conventional transgenic mice. In the case of the tetO BAC transgenic mice, EYFP induction in CA1 was dramatically increased, but expression in the dentate gyrus was still not observed. tetO knockin mice exhibited EYFP induction in both CA1 and the dentate gyrus, an expression profile consistent with that of αCaMKII promoter activity (Mayford et al., 1996). Crosses with other tTA lines, specific for orexin neurons (Orexin-tTA; A.Y., unpublished data), astrocytes (Mlc1-tTA; Tanaka et al., 2010), oligodendrocytes (PLP-tTA; Inamura et al., 2012), and microglia (Iba1-tTA; Figure S2), exhibited the same tendency: no/rare induction of EGFP in the tetO transgenic, moderate/high levels of EYFP expression in the tetO BAC transgenic, and the highest levels of expression in the tetO knockin mice. These observations indicated that both the genomic position of the tetO cassette and the method of genomic insertion were critical in gaining efficient gene induction. As the transgene
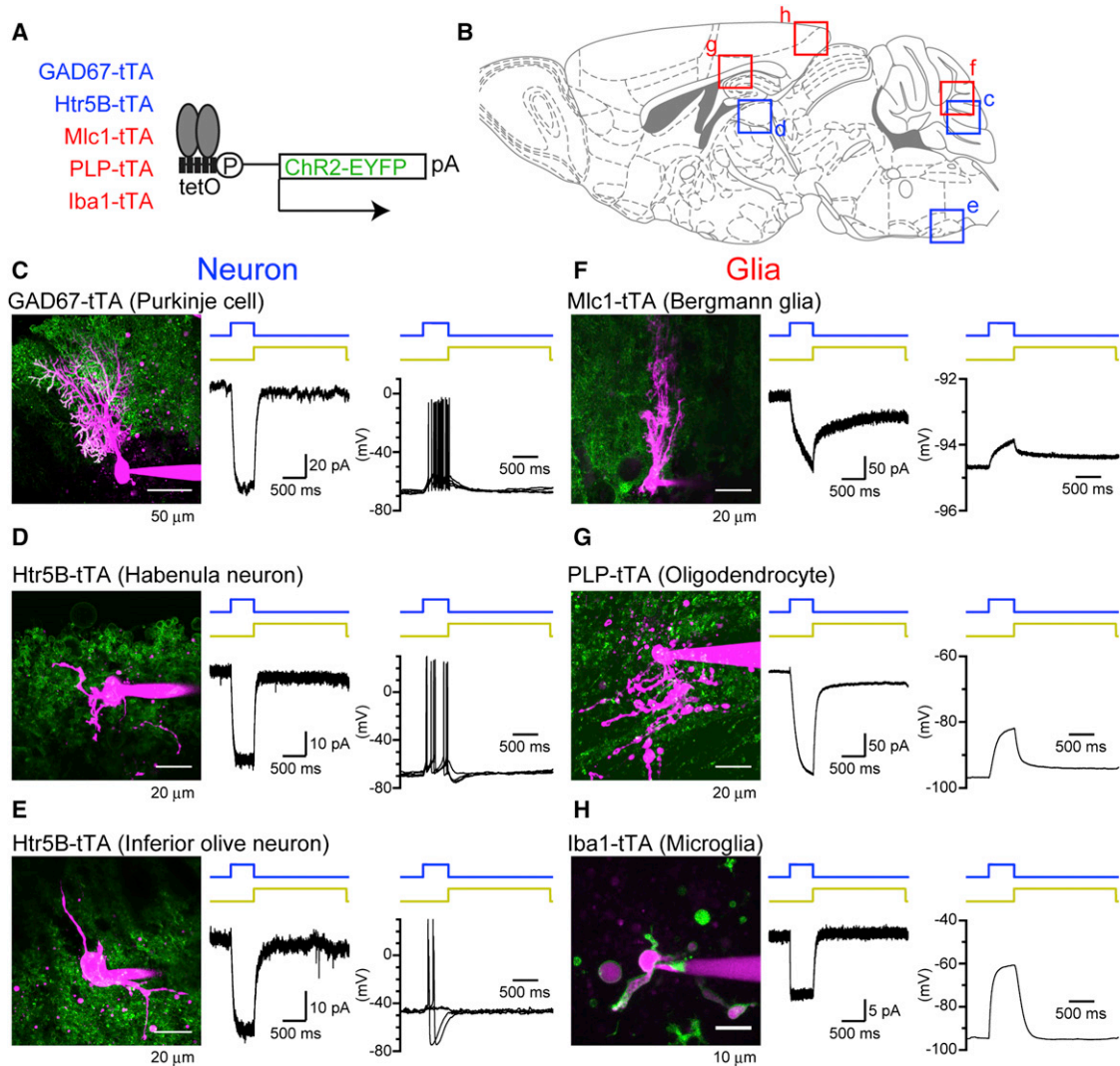
Figure 3. ChR2(C128S)-EYFP Expression Is High Enough to Permit Light-Evoked Responses in Multiple Cell Types
(A) Various promoter-tTA lines were crossed with our tetO-ChR2(C128S)-EYFP knockin mice.
(B) Anatomical location of the cells recorded in (C–H).
(C) GAD67-tTA drove ChR2(C128S)-EYFP expression in a subset of Purkinje cells (green) in the cerebellum. Using acute brain slices, cells with green fluorescence were visually selected and recorded in whole cell patch clamp mode with Alexa 594 in the pipette solution to confirm their identity from morphology (red). Illumination of blue light evoked inward current and yellow light resulted in cessation of this current (middle column; in voltage-clamp; Vh = −85 mV). Action potential firing was observed when recorded in current-clamp mode (right column; K$^+$-based internal solution; 5 traces overlaid).
(D and E) Htr5B-tTA drove ChR2(C128S)-EYFP expression in medial habenula and inferior olive neurons. In both cases, the inward current activated by the illumination was often sufficient to produce action potential firing.
(F–H) ChR2(C128S)-EYFP expression could also be driven in nonexcitable glial cells (astrocytes, oligodendrocytes, and microglia), and light-evoked current responses could be observed. Light-evoked depolarization was relatively small in astrocytes (cerebellar Bergman glial cells), likely due to the low input resistance and the lack of major voltage-dependent conductances.
See also Figures S2, S3, and S4.

insertion would occur randomly in conventional transgenic approach, it is possible to obtain ubiquitous high expression by pure chance. However, by knocking in the tetO cassette downstream of the β-actin gene, we have established the Knockin-mediated ENhanced Gene Expression by improved tetracycline-controlled gene induction (KENGE-tet) system for reliably generating transgenic mice with light-responsive cells.

Repertoire of Optogenetic Control of Neurons and Glial Cells

As we found that the KENGE-tet strategy greatly improved the expression level of the transgene, we next sought to determine whether the expression was high enough to drive cellular activity upon illumination (Figures 3C–3E). Use of the existing cell type-specific tTA lines, along with the tetO knockin mice, enabled

us to construct a repertoire of mice expressing ChR(C128S)-EYFP in a variety of tissues and cell types. We first prepared bigenic mice (P14-21) with a neuron-specific promoter driving tTA and performed whole cell patch-clamp recordings on cells expressing EYFP. Light-evoked responses of ChR2(C128S) from Purkinje cells in the cerebellum (with GAD67-tTA-mediated induction; generated by J.N. and Y.Y., see Extended Experimental Procedures), neurons in the medial habenula (serotonin receptor 5B-tTA [Htr5B-tTA]; Figure S3), and neurons in the inferior olive (Htr5B-tTA) were examined. In all cases, inward current (74.1 ± 49.7 pA, 16.1 ± 7.1 pA, and 29.9 pA in Purkinje cells, medial habenula neurons, and inferior olive neurons positive for EYFP; n = 4, 4, and 1, respectively) was evoked with blue light, and yellow light shut down the current, a feature of the bistable switch of ChR2(C128S). In most cases, the amount of photocurrent was sufficient to produce action potential firing in current clamp mode. Using slices from older animals (P30), we observed that the photocurrent was an order of magnitude larger in Purkinje cells positive for EYFP (Figure S4; P17–20, 52.9 ± 21.6 pA, P30, 582.7 ± 178.1 pA; n = 6 and 3, respectively). This implies that the ChR2(C128S)-EYFP expression progressively increases with age allowing robust control of cells' activity, especially in adult animals used for most in vivo studies. We also generated bigenic mice with a glia-specific promoter driving tTA and recorded light responses from the Bergmann glial cells (astrocytes) in the cerebellum (Mlc1-tTA) (Figure 3F), from oligodendrocytes in the hippocampal alveus (PLP-tTA) (Figure 3G), and from microglia in the caudal cortex (Iba1-tTA) (Figure 3H). Light-evoked current could also be induced in these glial cells, which are traditionally categorized as nonexcitable (104.5 ± 59.0 pA, 94.6 ± 35.7 pA, and 11.5 ± 2.4 pA for Bergmann glial cells, oligodendrocytes, and microglia positive for EYFP; n = 5, 6, and 5, respectively). The depolarization in astrocytes was relatively moderate, likely due to the low input resistance of these cells and the absence of major voltage-gated conductances.

In Vivo Optogenetic Control of Neurons

The benefit of our transgenic method is that we can obtain consistent ChR2(C128S)-EYFP expression patterns and levels within a given line of bigenic animals. In vivo experiments especially are often faced with variability between individual animals, and virus-mediated ChR2 expression would only add to the complexity of interpretation of the data, as the extent and localization of infection would inevitably vary between trials. The choice of the modified ChR2(C128S), which exhibits slow inactivation, seemed also advantageous in in vivo studies, as prolonged activation of cells is possible with only brief illumination with blue light, which should minimize the toxicity caused by the illumination itself. We took advantage of our system for the stable expression of ChR2(C128S)-EYFP and studied the light-evoked responses of neurons in vivo and the effect on the behavior of the animal.

For this study, we crossed a well-established tTA line, the αCaMKII-tTA line, with the tetO-ChR2(C128S)-EYFP knockin line that we generated (Figure 4A). The bigenic mice showed strong expression of ChR2(C128S)-EYFP in the hippocampal pyramidal neurons (Figure 2). Therefore, we first examined the effect of ChR2(C128S) activation on the field potential in the hippocampal CA1 area by in vivo recording using a microelectrode attached to an optical fiber (Figure 4A). Incidents of multi-unit and ripple-like synchronous events were prominently increased in response to blue light illumination (500-ms pulses, every 1 min; Figure 4B). As yellow light was not applied to rapidly terminate the ChR2(C128S) activation, the increase in the event frequency lasted for tens of seconds, but the event frequency came back close to the baseline within 1 min (Figure 4B, bottom), which allowed repetitive stimulation. These data show that the effect of the light stimulation on neuronal activity was clear and consistent (Figure 4B, n = 9 recordings from three animals).

To determine whether such manipulation of cell activity was powerful enough to cause behavioral responses, we implanted an optical fiber in position for illuminating the left, dorsal hippocampal CA1 area and connected it to a laser light source via an optical swivel to avoid tangling of the fiber from the free-moving mouse (Figure 4C). The mouse was kept in its home cage, and the mouse tended to stay in one location prior to the illumination. However, upon illumination (500-ms pulses, every 1 min), an increase in the mouse's locomotion activity occurred, along with an emergence of behavior resembling thigmotaxis. Seeking behavior, as well as digging of the bedding, was also observed. Interestingly, such behavior started with a delay of approximately 100 s, which contrasts with the direct ChR2 activation of neurons in the motor cortex, which causes muscle movements almost immediately upon illumination (Ayling et al., 2009; Hira et al., 2009). This suggests that the light stimulation in our case was not simply evoking motor behavior; some sort of cognitive response prior to the motor behavior could also have been evoked. Even though light pulses were periodically applied, the increase in locomotion activity gradually settled, which correlate with the moderate rundown of light-evoked neuronal activity with repetitive stimuli (Figure 4B). However, the increase was still observable after 30 min from the onset of illumination.

The mouse was sacrificed at 30 min after the initiation of illumination and processed for histochemical analyses (Figure 4D). It has been reported that increase in c-fos is related to cell activity (Schoenenberger et al., 2009; Sheng and Greenberg, 1990), and by using in situ hybridization, we revealed that unilateral 30 min activation of ChR2(C128S) in the hippocampal CA1 region resulted in bilateral increase in c-fos induction in neurons of the hippocampus. It is possible that diffuse light from the optic fiber directly stimulated the cells in the contralateral hippocampus; however, even though ChR2(C128S) was also expressed in the dorsal cortex through αCaMKII promoter activity, neurons in this region did not show significant increases in c-fos. Therefore, it is likely that excitation of neurons initiated unilaterally by illumination could have spread to the contralateral region by neural activity subsequent to the direct stimulation. In the wild-type mouse, no increase in c-fos expression or change in behavior was observed with illumination through an optic fiber placed similarly, showing that the neural activity was caused not by the possible heat from or the endogenous response to the illumination.

In contrast to the most previous transgenic approach in which only a weak expression was achieved in a small subset of cells, our KENGE-tet system achieves robust and strong
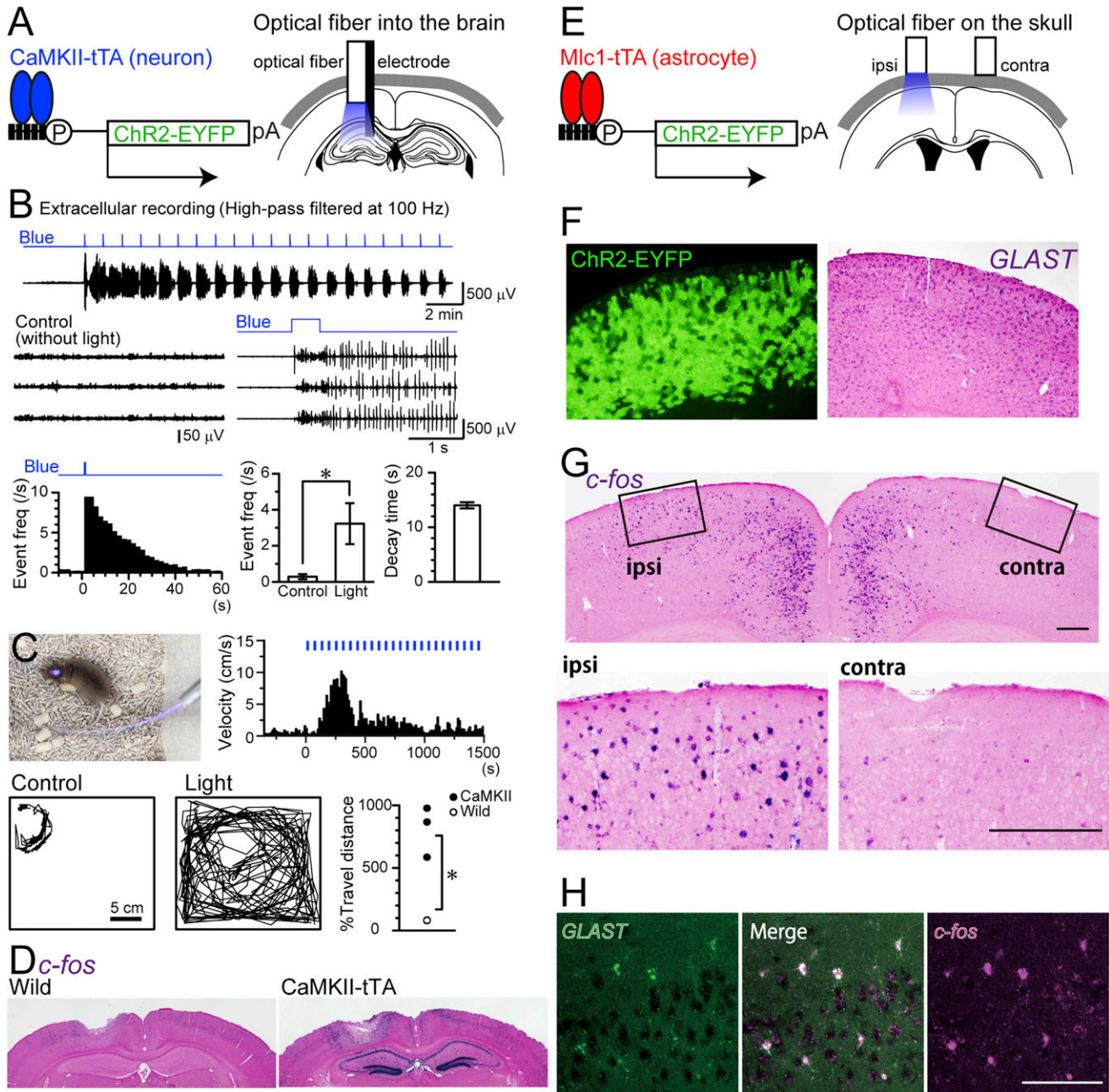
Figure 4. In Vivo Manipulations of Neurons and Glial Cells

(A) ChR2(C128S)-EYFP was expressed in hippocampal CA1 neurons by using the αCaMKII-tTA line. Dorsal left hippocampus was illuminated with blue light pulses (500 ms pulses, every 1 min for 20–25 min) through an optical fiber inserted into the brain, and neuronal activity was measured by an accompanying microelectrode.

(B) In vivo extracellular recordings of multi-unit and ripple-like activity of hippocampal neurons from an anesthesized transgenic mouse fixed under a stereotaxic apparatus. Representative three traces before and after illumination are magnified in the middle panels. (bottom left) Peri-stimulus time histogram of the ripple-like events from the example recording shown on top. Summary of the frequencies of ripple-like events during the 2 s leading up to (Control) and during the 2 s following (Light) the light illumination are shown in the bottom middle panel (n = 9 recordings from 3 animals; *p < 0.05, paired t test). (bottom right) Half decay time of the ripple-like event frequency from the stimulus onset. Error bars: SEM.

(C) A photo of a freely moving mouse in its home cage with an optical fiber inserted into its brain close to the hippocampus (top left). Representative data of the tracking of the head position (1 s intervals; bottom) during the 6 min period prior to (Control) and the 6 min period after (Light) the onset of a blue light stimulus train (500 ms pulses at 1 min intervals). Locomotion velocity is plotted against time (bin width = 10 s; top right). Blue bars on top represent the timing of the light stimuli. Bottom left panel shows the summary of the total travel distance during the 25 min after the initiation of light illumination train (n = 2 and 3 for transgenic and wild mice, respectively; *p < 0.05, Student's t test).

ChR2(C128S)-EYFP expression. The above data demonstrate that the expression is high enough that consistent changing of the neuronal firing is possible and artificial manipulation of the circuit can be strong enough to manifest in behavioral response and in *c-fos* expression.

Optogenetic Manipulation of Glial Cells

Stimulation of neurons is often realized by using extracellular electrodes in electrophysiological studies, but what is often overlooked is that such stimulation inevitably stimulates the nearby glial cells as well. To understand how glial cells interact with neurons and participate in information processing in the brain, specific stimulation of glial cells is desirable. To this end, optogenetic manipulation of glial cell activity would be ideal; however, we were uncertain whether current injection through ChR2(C128S) would be sufficient to change glial cell activity status. Depolarization by current injection through ChR2(C128S) by itself is not surprising as any cell should react in this way (Figures 3F and 3G). Therefore, we used our astrocyte-specific ChR2(C128S)-EYFP-expressing mice, the Mlc1-tTA::tetO-ChR2(C128S)-EYFP knockin mice, and examined whether light stimulation could promote *c-fos* mRNA induction in astrocytes (Figure 4, right).

When studying glial cells, one needs to remember that these cells are very sensitive to injury. For example, just the insertion of an optical plastic fiber resulted in gliosis around the fiber and blue light illumination resulted in *c-fos* induction in glial cells beneath the fiber in wild-type mice, which have no expression of ChR2(C128S)-EYFP (data not shown). It is possible that local heat produced by the illumination (Yizhar et al., 2011) could have induced the *c-fos* expression in the injured glial cells (Dragunow et al., 1989). This result indicates that surgical operation should be avoided when studying the physiological roles of glial cell activity; therefore, the use of transgenic expression of ChR2 is preferred over virus mediated gene transfer. Our choice of the modified ChR2, ChR2(C128S). was also ideal because this ChR2 mutant is highly sensitive to light; therefore, the chance of stimulating this ChR2 variant through the skull without optical fiber insertion was high.

An optical plastic fiber was placed on top of the skull and fixed with dental cement, and the brain was illuminated only through the skull (Figure 4E). Such manipulation alone did not produce any injury to the brain or *c-fos* induction (data not shown). The induction of *c-fos* mRNA in cortical astrocytes was confirmed at 30 min after the onset of illumination (500-ms pulses, every 10 s; Figures 4G and 4H). *c-fos* mRNA induction in astrocytes was never observed in wild-type mice after illumination through

the skull, and induction was reproducibly observed in the bigenic mice, indicating that this manipulation is specific. We also checked the expression of *c-fms* mRNA, which gets increased in activated microglial cells, and found that the expression level was not increased surrounding the operated and illuminated area (data not shown). This confirms that our light illumination protocol itself did not induce specific damage to the brain tissue.

Our research shows that *c-fos* induction in astrocytes is manipulable by optogenetics. Two recent studies showed optogenetic tool expression either in cultured astrocytes (Li et al., 2012) or in astrocytes in vivo using viral delivery of the transgene (Gourine et al., 2010); however, our method is unique, as whole animals expressing ChR2(C128S) were obtained, allowing low-invasiveness in vivo experiments. We have yet to understand the mechanistic pathway leading from ChR2(C128S)-mediated current influx to *c-fos* induction; however, the results show that ChR2(C128S) activation could be used as a tool to specifically manipulate astrocyte activity and the trace of manipulation can be pursued by *c-fos* histochemistry.

DISCUSSION

Our initial attempts, as well as those of some of our colleagues, to express ChR2 in a cell type-specific manner at sufficiently high levels to accomplish optogenetic manipulation of cell activity using the transgenic approach have largely failed because achievement of both specific and abundant expression was difficult. We have provided a solution to these conflicting requirements by using the improved KENGE-tet system. Specificity in this system was attained by preparing a panel of tissue-specific tTA lines, which allow cell type-specific expression in various cell types. It has also been reported that the bipartite tet system can amplify the level of transgene expression much more than direct connection of the cell type-specific promoter to the transgene (Arenkiel et al., 2007; Dhawale et al., 2010; Tomita et al., 2009; Wang et al., 2007). In addition, knocking in our transgene, ChR2(C128S)-EYFP, into a locus just downstream of β-actin allowed sufficiently high induction for light responses.

The keys to our success of achieving high levels of gene induction by the KENGE-tet system were that: (1) the tetO was inserted to the genome as "knockin" and (2) the targeted locus of the "knockin" was strategically selected. TetO mice generated by conventional plasmid transgenic approach would cause transgene to insert in more or less random locations and tTA-mediated gene induction in these mice often fails presumably due to chromosomal position effects. We have already shown in our previous study that tetO knockin yielded a high level of

---

(D) ChR2(C128S)-mediated unilateral activation of CA1 neurons resulted in *c-fos* mRNA induction bilaterally in both CA1 and dentate gyrus neurons.

(E) Astrocytic ChR2(C128S)-EYFP expression was induced by using the Mlc1-tTA line. To avoid injury-induced glial cell activation, the optical fibers were placed on top of the skull. Light was sent through only one of the two fibers.

(F) Cortical astrocytes, which were labeled by in situ hybridization to GLAST mRNA (right), expressed EYFP (left), confirming the expression of ChR2(C128S)-EYFP in astrocytes.

(G) Illumination through the skull was able to induce *c-fos* mRNA expression only on the ipsi-lateral side (left), to which the light stimulus was given, and no expression was observed in the contralateral side (right). The medial region of the cortex also expressed *c-fos* but such *c-fos* expression was also observed in wild-type or in mice not stimulated with light, thus, this expression was endogenous to the mice kept in our environment and not related to ChR2(C128S) activation.

(H) The *c-fos* mRNA positive cells stimulated by light were found to express GLAST mRNA, indicating that *c-fos* was induced in astrocytes. Scale bars: 200 μm. See also Figure S4.

transactivation (Tanaka et al., 2010). In the current study, to avoid the chromosomal position effects as much as possible, genomic loci where the tetO promoter is activatable by the tTA produced were searched. Previous studies have reported that several loci, including the TIGRE locus (chr9, between AB124611 and *Carm1* genes) (Zeng et al., 2008), the LC-1 locus (chr6, between *Vmn1r33* and *Vmn1r34* genes) (Schönig et al., 2011), and the *HPRT* locus (chr X) (Palais et al., 2009), provide high tTA-mediated transcription when the tetO promoter is inserted. *HPRT* is generally regarded as a housekeeping gene, motivating us to select another housekeeping gene, in this case the gene for β-actin, for our gene targeting.

Once the targeted locus was selected, the BAC transgenic strategy could be used to avoid a chromosomal position effect (Schönig et al., 2011). However, we assumed that tetO knockin by ES cell homologous recombination would yield an even higher level of transactivation than did the BAC transgenic strategy, according to our experience with tetO knockin mice (Tanaka et al., 2010). In the current study, we performed a direct comparison between BAC transgenic and knockin approaches, and we showed that the knockin of tetO into downstream of housekeeping gene provided improvement to the tet system, although the underlying mechanism of the enhancement of expression was not made clear. We do need to note that in some cases where the endogenous promoter activity is extremely high, such as the orexin and PLP promoters, abundant tTA expression levels are attained. In such cases, BAC transgenic approach with tetO inserted downstream of house-keeping gene within BAC provides high enough levels of ChR2 (Figure 2) to trigger photocurrents (data not shown). However, many endogenous promoters that are specific to a certain population of cells usually do not have such a high activity, and, in such case, only low to moderate tTA levels could be attained, resulting low levels of ChR2 induction. According to numbers of trials that we tested, only the tetO knockin strategy, the KENGE-tet system, reliably produced high levels of gene induction.

In addition to our improved KENGE-tet system for ChR2(C128S)-EYFP expression, there are two other genetic approaches to the induction of cell type-specific ChR2 expression in mice published to date: the ChR2 BAC transgenic approach (Hägglund et al., 2010; Zhao et al., 2011) and Cre-loxP-mediated ChR2 expression (Kätzel et al., 2011; Madisen et al., 2012). Maintenance of ChR2 BAC transgenic mice is the easiest among the three approaches, as only a single line of mice needs to be kept. However, unlike the tet system approach, simple BAC transgenic strategy lacks gene amplification modules, and thus this strategy often requires strong endogenous promoter activity. There are five successful, published cases of the use of the ChR2 BAC transgenic approach; these used vesicular glutamate transporter 2 (vGluT2) (Hägglund et al., 2010), vesicular gamma aminobutyric acid (GABA) transporter (VGAT), choline acethyltransferase (ChAT), tryptophan hydroxylase-2 (Tph2), and parvalbumin, (Pvalb) (Zhao et al., 2011) promoters. In all cases, expression of the mRNAs encoding these proteins is high, indicating that these promoters have very strong activity. If cell type-specific marker gene expression were weak, the BAC transgenic strategy may not achieve enough ChR2 expression for optogenetic manipulation, although

other strategies could be sought in addition to the BAC strategy to compensate for the weak promoter activity.

The advantage of the Cre-loxP and tet system-mediated strategies is that a panel of cell type-specific Cre and tTA lines already exists. Both systems are also equipped with gene amplification modules. The Cre-loxP system utilizes the CMV early enhancer/chicken β-actin (CAG) promoter in the ROSA locus, and the tet system utilizes the tTA-dependent promoter; both promoters can strongly drive gene induction. One drawback of the Cre-loxP system is that it has been reported that even with the ChR2 transgene located at the ROSA locus with the CAG promoter, homozygosity was required to induce sufficient expression of ChR2 to drive action potential firing specifically in cortical interneurons (Kätzel et al., 2011). That being said, both the Cre-loxP and tet systems are ideal in achieving both specificity and amplification of ChR2 expression. Our choice of the modified ChR2(C128S) as a target transgene was also advantageous for optogenetic control of cell activity because of the higher sensitivity to light and the shorter illumination time required for long-term ChR2 activation.

As shown in this study, our KENGE-tet system is applicable to optogenetic manipulation of not only excitable neurons but also "nonexcitable" glial cells. We demonstrated that ChR2(C128S)-mediated inward currents resulted in *c-fos* mRNA induction in astrocytes. We also observed *c-fos* mRNA induction in oligodendrocytes in PLP-tTA::tetO-ChR2(C128S)-EYFP knockin mice after illumination (data not shown). These results indicate that ChR2(C128S) activation can be used as a tool to change the status of nonexcitable cells and that the change in their activity can be traced by *c-fos* induction.

Optogenetic manipulation of nonexcitable cells outside the nervous system could also be used to understand cell type-specific functionality in various tissues. For example, we have noticed that tissue macrophages—osteoclasts in bone, Kupffer cells in liver, and alveolar macrophages in lung—all express ChR2(C128S)-EYFP in Iba1-tTA::tetO-ChR2(C128S)-EYFP knockin mice (data not shown). For driving the activity of these nonexcitable cells, in addition to ChR2(C128S), Ca^{2+}-permeable ChR2 (Kleinlogel et al., 2011) could be used for Ca^{2+} induction and photoactivated adenylate cyclase (Schröder-Lang et al., 2007) could be used for cAMP induction. Construction of a panel of tetO knockin lines, including the above-mentioned light-sensitive proteins, will add options for optogenetic manipulation of cell function in both excitable and nonexcitable cells and facilitate research in many fields.

EXPERIMENTAL PROCEDURES

Generation of Transgenic Mice

Detailed information of generating tetO-ChR2(C128S)-EYFP BAC transgenic mice, tetO-ChR2(C128S)-EYFP knockin mouse, Iba1-tTA mouse, Htr5B-tTA mouse, and GAD67-tTA mouse is available in the Extended Experimental Procedures. A schematic diagram indicating the targeting vector for tetO-ChR2(C128S)-EYFP is given in Figure S1. Basic characterization of Iba1-tTA and Htr5B-tTA mice is shown in Figures S2 and S3. Information regarding αCaMKII-tTA (Mayford et al., 1996), BTR6 (Chuhma et al., 2011), Mlc1-tTA (Tanaka et al., 2010), and PLP-tTA (Inamura et al., 2012) mice are already published. Information regarding Orexin-tTA mouse (generated by A.Y.) is unpublished. Genotyping primers are also given in the Extended Experimental Procedures.

Immunohistochemistry and In Situ Hybridization

Standard procedures were taken for immunohistochemistry and the antibodies used and the reaction times are given in detail in the Extended Experimental Procedures. The in situ hybridization method was as described previously (Ma et al., 2006) and written briefly in the Extended Experimental Procedures.

Acute Brain Slice Preparations and Patch-Clamp Recordings

Brain slices were prepared from mice aged P14–P21, unless otherwise noted. Slices were cut at a thickness of 250–400 μm using a microslicer and the slices were transferred to a submerged-type recording chamber and continuously superfused. All recordings were performed at room temperature (22–25°C). Visually identified cells were voltage clamped at –70 mV in whole-cell patch clamp mode. High-power blue LED (470 nm; 8 mW at sample location) was placed underneath the condenser lens of the upright microscope for full-field activation of ChR2(C128S) and yellow light, filtered (560 nm center 14 nm band-pass filter; 0.15 mW at sample location) from a mercury lamp, was directed through the epifluorescence port for closing of the ChR2(C128S).

In Vivo Electrophysiological Recording and Optical Stimulation

Each mouse was anesthetized with ketamine hydrochloride (100 mg/kg body weight, i.p.) and xylazine hydrochloride (5 mg/kg body weight, i.p.). The skull was widely exposed and a small U-frame holder was attached for head fixation. After recovery from the surgery (2 or 3 days later), the mouse was positioned in a stereotaxic apparatus with its head restrained using the U-frame holder under light anesthesia with ketamine hydrochloride (50–100 mg/kg body weight, i.p.). A part of the skull in one hemisphere was removed to access the hippocampus. For recording neural activity while illuminating with blue light, a glass-coated Elgiloy microelectrode (0.5–1.0 MΩ at 1 kHz), along with a 50 μm diameter optical fiber, was inserted perpendicularly into the brain through the dura mater using a hydraulic microdrive. A 50 mW blue laser was coupled to an optical fiber. The target area was 2.0–3.0 mm posterior and 1.5–3.0 mm lateral to bregma and 1.2–1.6 mm deep from the brain surface for the hippocampus (Franklin and Paxinos, 2008).

In Vivo Optical Stimulation in Freely Moving Mice

Violet light was generated by laser diode (445 nm, 400 mW) and applied through plastic optical fibers (0.5 mm diameter). An optical swivel (COME2, Lucir, Tsukuba, Japan) was used for unrestricted in vivo illumination. Violet light power intensity at the tip of the plastic fiber was 6.7 mW/mm^2. For hippocampal CA1 pyramidal neuron stimulation, a plastic optical fiber was inserted above the left dorsal hippocampus using a stereotaxic frame with the tip of the fiber located at 2.0 mm posterior, 1.5 mm lateral to bregma, and 1 mm deep from the skull. The fiber was fixed on the skull using dental cement. For astrocyte stimulation, the plastic fiber was placed on top of the skull (0.5 mm anterior and 1.5 mm lateral to bregma) and fixed with the dental cement. The mice were allowed to recover for at least one week after fiber implantation. For hippocampal neuron stimulation, 500 ms illumination was given every 1 min in the home cage, and locomotive activity was captured with a video camera. For astrocyte stimulation, 500 ms illumination was given every 10 s in the home cage. Details for all physiological and behavioral experiments are also described in the Extended Experimental Procedures.

Resource

tetO-ChR2(C128S)-EYFP BAC transgenic (Reference number: RBRC05453), tetO-ChR2(C128S)-EYFP knockin (RBRC05454), Mlc1-tTA(RBRC05450), PLP-tTA (RBRC05446), and Htr5B-tTA (RBRC05445) are available from RIKEN Bioresource Center in Japan.

SUPPLEMENTAL INFORMATION

Supplemental Information includes Extended Experimental Procedures and four figures and can be found with this article online at http://dx.doi.org/10.1016/j.celrep.2012.06.011.

REFERENCES

Arenkiel, B.R., Peca, J., Davison, I.G., Feliciano, C., Deisseroth, K., Augustine, G.J., Ehlers, M.D., and Feng, G. (2007). In vivo light-induced activation of neural circuitry in transgenic mice expressing channelrhodopsin-2. Neuron 54, 205–218.

Ayling, O.G., Harrison, T.C., Boyd, J.D., Goroshkov, A., and Murphy, T.H. (2009). Automated light-based mapping of motor cortex by photoactivation of channelrhodopsin-2 transgenic mice. Nat. Methods 6, 219–224.

Berndt, A., Yizhar, O., Gunaydin, L.A., Hegemann, P., and Deisseroth, K. (2009). Bi-stable neural state switches. Nat. Neurosci. 12, 229–234.

Boyden, E.S., Zhang, F., Bamberg, E., Nagel, G., and Deisseroth, K. (2005). Millisecond-timescale, genetically targeted optical control of neural activity. Nat. Neurosci. 8, 1263–1268.

Chuhma, N., Tanaka, K.F., Hen, R., and Rayport, S. (2011). Functional connectome of the striatal medium spiny neuron. J. Neurosci. 31, 1183–1192.

Dhawale, A.K., Hagiwara, A., Bhalla, U.S., Murthy, V.N., and Albeanu, D.F. (2010). Non-redundant odor coding by sister mitral cells revealed by light addressable glomeruli in the mouse. Nat. Neurosci. 13, 1404–1412.

Dragunow, M., Currie, R.W., Robertson, H.A., and Faull, R.L. (1989). Heat shock induces c-fos protein-like immunoreactivity in glial cells in adult rat brain. Exp. Neurol. 106, 105–109.

Gossen, M., Freundlieb, S., Bender, G., Müller, G., Hillen, W., and Bujard, H. (1995). Transcriptional activation by tetracyclines in mammalian cells. Science 268, 1766–1769.

Gourine, A.V., Kasymov, V., Marina, N., Tang, F., Figueiredo, M.F., Lane, S., Teschemacher, A.G., Spyer, K.M., Deisseroth, K., and Kasparov, S. (2010). Astrocytes control breathing through pH-dependent release of ATP. Science 329, 571–575.

Hägglund, M., Borgius, L., Dougherty, K.J., and Kiehn, O. (2010). Activation of groups of excitatory neurons in the mammalian spinal cord or hindbrain evokes locomotion. Nat. Neurosci. 13, 246–252.

Hira, R., Honkura, N., Noguchi, J., Maruyama, Y., Augustine, G.J., Kasai, H., and Matsuzaki, M. (2009). Transcranial optogenetic stimulation for functional mapping of the motor cortex. J. Neurosci. Methods 179, 258–263.

Inamura, N., Sugio, S., Macklin, W.B., Tomita, K., Tanaka, K.F., and Ikenaka, K. (2012). Gene induction in mature oligodendrocytes with a PLP-tTA mouse line. Genesis *50*, 424–428.

Kätzel, D., Zemelman, B.V., Buetfering, C., Wölfel, M., and Miesenböck, G. (2011). The columnar and laminar organization of inhibitory connections to neocortical excitatory cells. Nat. Neurosci. *14*, 100–107.

Kleinlogel, S., Feldbauer, K., Dempski, R.E., Fotis, H., Wood, P.G., Bamann, C., and Bamberg, E. (2011). Ultra light-sensitive and fast neuronal activation with the $Ca^{2}+$-permeable channelrhodopsin CatCh. Nat. Neurosci. *14*, 513–518.

Li, D., Hérault, K., Isacoff, E.Y., Oheim, M., and Ropert, N. (2012). Optogenetic activation of LiGluR-expressing astrocytes evokes anion channel-mediated glutamate release. J. Physiol. *590*, 855–873.

Madisen, L., Mao, T., Koch, H., Zhuo, J.M., Berenyi, A., Fujisawa, S., Hsu, Y.W., Garcia, A.J., 3rd, Gu, X., Zanella, S., Kidney, J., Gu, H., Mao, Y., Hooks, B.M., Boyden, E.S., Buzsáki, G., Ramirez, J.M., Jones, A.R., Svoboda, K., Han, X., Turner, E.E., and Zeng, H. (2012). A toolbox of Cre-dependent optogenetic transgenic mice for light-induced activation and silencing. Nat. Neurosci. *15*, 793–802.

Mayford, M., Bach, M.E., Huang, Y.Y., Wang, L., Hawkins, R.D., and Kandel, E.R. (1996). Control of memory formation through regulated expression of a CaMKII transgene. Science *274*, 1678–1683.

Nagel, G., Szellas, T., Huhn, W., Kateriya, S., Adeishvili, N., Berthold, P., Ollig, D., Hegemann, P., and Bamberg, E. (2003). Channelrhodopsin-2, a directly light-gated cation-selective membrane channel. Proc. Natl. Acad. Sci. USA *100*, 13940–13945.

Oyer, J.A., Chu, A., Brar, S., and Turker, M.S. (2009). Aberrant epigenetic silencing is triggered by a transient reduction in gene expression. PLoS ONE *4*, e4832.

Palais, G., Nguyen Dinh Cat, A., Friedman, H., Panek-Huet, N., Millet, A., Tronche, F., Gellen, B., Mercadier, J.J., Peterson, A., and Jaisser, F. (2009). Targeted transgenesis at the HPRT locus: an efficient strategy to achieve tightly controlled in vivo conditional expression with the tet system. Physiol. Genomics *37*, 140–146.

Schoenenberger, P., Gerosa, D., and Oertner, T.G. (2009). Temporal control of immediate early gene induction by light. PLoS ONE *4*, e8185.

Schönig, K., Kentner, D., Gossen, M., Baldinger, T., Miao, J., Welzel, K., Vente, A., Bartsch, D., and Bujard, H. (2011). Development of a BAC vector for integration-independent and tight regulation of transgenes in rodents via the Tet system. Transgenic Res. *20*, 709–720.

Schröder-Lang, S., Schwärzel, M., Seifert, R., Strünker, T., Kateriya, S., Looser, J., Watanabe, M., Kaupp, U.B., Hegemann, P., and Nagel, G. (2007). Fast manipulation of cellular cAMP level by light in vivo. Nat. Methods *4*, 39–42.

Sheng, M., and Greenberg, M.E. (1990). The regulation and function of c-fos and other immediate early genes in the nervous system. Neuron *4*, 477–485.

Steriade, M., Nuñez, A., and Amzica, F. (1993). A novel slow (< 1 Hz) oscillation of neocortical neurons in vivo: depolarizing and hyperpolarizing components. J. Neurosci. *13*, 3252–3265.

Tanaka, K.F., Ahmari, S.E., Leonardo, E.D., Richardson-Jones, J.W., Budreck, E.C., Scheiffele, P., Sugio, S., Inamura, N., Ikenaka, K., and Hen, R. (2010). Flexible Accelerated STOP Tetracycline Operator-knockin (FAST): a versatile and efficient new gene modulating system. Biol. Psychiatry *67*, 770–773.

Tomita, H., Sugano, E., Fukazawa, Y., Isago, H., Sugiyama, Y., Hiroi, T., Ishizuka, T., Mushiake, H., Kato, M., Hirabayashi, M., et al. (2009). Visual properties of transgenic rats harboring the channelrhodopsin-2 gene regulated by the thy-1.2 promoter. PLoS ONE *4*, e7679.

Wang, H., Peca, J., Matsuzaki, M., Matsuzaki, K., Noguchi, J., Qiu, L., Wang, D., Zhang, F., Boyden, E., Deisseroth, K., et al. (2007). High-speed mapping of synaptic connectivity using photostimulation in Channelrhodopsin-2 transgenic mice. Proc. Natl. Acad. Sci. USA *104*, 8143–8148.

Yizhar, O., Fenno, L.E., Davidson, T.J., Mogri, M., and Deisseroth, K. (2011). Optogenetics in neural systems. Neuron *71*, 9–34.

Zeng, H., Horie, K., Madisen, L., Pavlova, M.N., Gragerova, G., Rohde, A.D., Schimpf, B.A., Liang, Y., Ojala, E., Kramer, F., Roth, P., Slobodskaya, O., Dolka, I., Southon, E.A., Tessarollo, L., Bornfeldt, K.E., Gragerov, A., Pavlakis, G.N., and Gaitanaris, G.A. (2008). An inducible and reversible mouse genetic rescue system. PLoS Genet. *4*, e1000069.

Zhao, S., Ting, J.T., Atallah, H.E., Qiu, L., Tan, J., Gloss, B., Augustine, G.J., Deisseroth, K., Luo, M., Graybiel, A.M., and Feng, G. (2011). Cell type–specific channelrhodopsin-2 transgenic mice for optogenetic dissection of neural circuitry function. Nat. Methods *8*, 745–752.

Zhu, P., Aller, M.I., Baron, U., Cambridge, S., Bausen, M., Herb, J., Sawinski, J., Cetin, A., Osten, P., Nelson, M.L., Kügler, S., Seeburg, P.H., Sprengel, R., and Hasan, M.T. (2007). Silencing and un-silencing of tetracycline-controlled genes in neurons. PLoS ONE *2*, e533.

Supplemental Information

EXTENDED EXPERIMENTAL PROCEDURES

All animal procedures were conducted in accordance with the National Institutes of Health Guide for the Care and Use of Laboratory Animals and approved by the Animal Research Committee of the National Institute for Physiological Sciences.

Generation of tetO-ChR2(C128S)-EYFP BAC Transgenic Mice

We constructed the plasmid containing the tetO-ChR2(C128S)EYFP polyA cassette with the Neo selection gene flanked on both sides by FRT sites in which the following elements were connected in tandem: tetO sequence, rabbit β globin intron, ChR2(C128S)EYFP cDNA, SV40 polyadenylation signal, FRT-flanked PGK-EM7-Neo. To insert the above cassette downstream of the mouse β-actin gene, a 370 bp of 5′ homology arm, consisting of 340 bp upstream of the mouse β-actin gene polyadenylation signal (AATAAA) and 30 bp downstream of the AATAAA sequence, was connected to the 5′ end of the tetO sequence; and a 310 bp 3′ homology arm, consisting of the sequence from 31 to 340 bp downstream of the AATAAA sequence, was connected to the 3′ end of Neo. To perform BAC recombination, DNA fragments with both homology arms were electroporated into bacteria carrying the BAC (clone RP23-289L7) and the pBADTcTypeG plasmid (a gift from Dr. Manabu Nakayama, Kazusa Institute, Japan) (Nakayama and Ohara, 2005). Kanamycin-resistant clones were selected as the modified BAC and tetO-ChR2(C128S)-EYFP polyA cassette was subsequently inserted 30 bp downstream of mouse β-actin gene AATAAA. Linearized modified BAC DNA with PI-SceI was injected into fertilized eggs from C57BL6 mice and 3 founders were established. All founders were crossed with ROSA-Flpe mice (Farley et al., 2000) to remove the FRT-flanked Neo selection marker. We selected one line exhibiting the best transactivation, as determined by crossing with αCaMKII-tTA, and established this line as the tetO-ChR2(C128S)-EYFP BAC transgenic mouse line.

Generation of tetO-ChR2(C128S)-EYFP Knockin Mice

The targeting vector was isolated from the kanamycin-resistant, modified BAC clone by using a retrieval technique involving insertion into the pMCS-DTA plasmid (gift from Dr. Kosuke Yusa, Osaka University, Japan). We subsequently obtained a targeting vector comprised of a 10 kb 5′ homology arm, tetO-ChR2(C128S) polyA cassette with Neo, a 1.9 kb 3′ homology arm, and diphtheria toxin A subunit (DTA) (Figure S1A). B6/129 ES cells (line G0G1) were used. We obtained six recombinant clones out of ninety-six G418-resistant clones. Recombination was confirmed by Southern blotting with 400 bp 3-prime outside probe, which recognized a 5.6 kb fragment of the wild-type allele and a 3.8 kb fragment of the targeted allele in genomic DNA digested with NcoI (Figure S1B). Germline transmitted offspring were established as tetO-ChR2(C128S)EYFP-Neo knock-in mice. tetO-ChR2(C128S)-EYFP-Neo mice were crossed with ROSA-Flpe mice, and FRT-flanked Neo selection marker were removed. tetO-ChR2(C128S)-EYFP knockin mice were subsequently generated.

Generation of Iba1-tTA Mouse and Characterization

We modified 2 kb mouse Iba1 promoter (Hirasawa et al., 2005). The original Iba1 promoter contains exon 1, which has the translation initiation site, and exon 2, thus the connected target gene yields protein with N-terminal Iba1 peptide. To avoid the addition of Iba1 peptide to tTA, we replaced ATG with TGT. This modification resulted in the disruption of original translation initiation site to enable translation of the target gene per se. We generated lenti virus carrying modified Iba1 promoter-EGFP and transfected this virus to primary cultured microglia in which Iba1 gene was constitutively expressed. We observed EGFP expression in transfected microglia and thus concluded that the modified Iba1 promoter was able to apply transgene induction in microglia as well as the original promoter. We constructed the 3.1 kb DNA fragment containing modified 2 kb mouse Iba1 promoter, mammalianized tTA (Inamura et al., 2012), and SV40 polyA (Figure S2A), and injected the DNA fragment into fertilized mouse eggs from the C57BL6/J strain. We generated two different founders: lines 54 and 75. Bigenic mice with Iba1-tTA and tetO-ChR2(C128S)-EYFP knockin were used for immunohistochemistry of EYFP. Both lines showed EYFP induction only in Iba1 positive microglia (line 54: 68% of Iba1 positive cells (n = 250, in the hippocampus) expressed EYFP; line 75: 88% of Iba1 positive cells (n = 225)) (Figure S2C). Direct EYFP fluorescence induced by line 54 was higher than that by line 75. Line 54 was used in slice physiology in Figure 3.

Generation of Htr5B-tTA Mouse and Characterization

We used a pL452 (gift from Dr. Neal Copeland, National Cancer Institute, USA), in which the following elements were connected in tandem: multicloning site1 (SacII/NotI/BamHI), loxP, PGK-EM7-Neo minigene (reverse orientation), loxP, multicloning site2 (EcoRI/KpnI). 400 bp of DNA fragments both upstream and downstream of the Htr5B translation initiation site were amplified with PCR primers containing appropriate restriction enzyme sites (SacI/NotI and EcoRI/KpnI), and respectively inserted into each multicloning site of the pL452 plasmid. Mammalianized tTA (mtTA)-rabbit beta globin polyA signal fragment was inserted into NotI/BamHI site of above modified pL452 plasmid, resulting that the start codon of the mtTA was placed exactly over the start codon of Htr5B. In order to perform BAC recombination, the mtTA-polyA-Neo cassette with 400 bp homology arms was transferred into the bacteria carrying the BAC (clone RP23-122O2) and the pBADTcTypeG plasmid. The targeting vector was isolated from the recombined, kanamycin-resistant BAC clone by using a retrieving technique into pMCS-DTA plasmid. We subsequently obtained a targeting vector comprised of diphtheria toxin A subunit (DTA), 2.2 kb 5-prime homology arm, mtTA-polyA-Neo cassette, and 9.6 kb 3-prime homology arm (Figure S3A). The targeting vector was linearized with PacI, followed by the electroporation into 129 SvEv ES cells (line CSL3). G418 resistant clones were screened by Southern blotting with 400 bp 5-prime outside probe, which recognized

a 6.7 kb fragment of the wild-type allele and a 11 kb fragment of the targeted allele in genomic DNA digested with HindIII (Figure S3B). Targeted ES cells were injected into blastcysts from C57BL6 mice to generate chimeras. Germline transmitted offspring were crossed with EIIa-Cre mice (Lakso et al., 1992), and loxP flanking Neo sequences were removed. In situ hybridization was performed to examine mtTA mRNA expression under the control of Htr5B promoter (Figure S3C). Bigenic mice with Htr5B-tTA and tetO-ChR2(C128S)-EYFP knockin were used for immunohistochemistry of EYFP in order to examine where tTA-mediated gene induction took place (Figure S3D).

Generation of the GAD67-tTA Mouse

tTA2 is tetracycline-controlled transactivator containing modified VP16 activation domains (Baron et al., 1997). A cassette containing the tTA2 cDNA started from the second codon, the SV40 polyadenylation signal and loxP-flanked Neo selection marker (PGK-Neo), was inserted into the third codon of a plasmid containing exon 1 of the *GAD67* locus. The targeting vector contained a 6.5 kb homologous GAD67 genomic DNA, with 5.0 kb located 5′ and 2.1 kb located 3′ to the tTA2 cDNA and PGK-Neo gene, respectively. DTA gene (pMC1DT-ApA) was included in the targeting vector for negative selection. The linearized targeting vector was electroporated into ES cells. G418-resistant recombinant ES cells were used to generate chimeras. Germline transmitted offspring were established as GAD67-tTA with PGK-Neo knock-in mice. The GAD67-tTA knock-in mice were generated by mating with EIIa-Cre mice to remove loxP-flanked Neo selection marker.

Mouse Genotyping

The following PCR primer sets were used in mouse genotyping: ChR2F (5′-CATCCTTATCCACCTGAGCAAC-3′) and ChR2R (5′-ACCGACCCTTTGGCACAGTATG-3′) for tetO-ChR2(C128S) and BTR6 mice; NNU (5′- aggcttgagatctggccatac-3′) and XZTL (5′-aagggcaaaagtgagtatggtg-3′) for αCaMKII-tTA mice; MlcU-657 (5′-AAATTCAGGAAGCTGTGTGCCTGC-3′) and mtTA24L (5′-cggagttgatcaccttggacttgt-3′) for Mlc1-mtTA mice; Ox up (5′-GCAGCGGCCATTCCTTGG-3′) and mtTA24L for orexin-mtTA mice; PLPU-604 (5′-tttcccatggtctcccttgagctt-3′) and mtTA24L for PLP-mtTA mice; Iba1552U (5′-atccctgggagttagcaagggaat-3′) and mtTA24L for Iba1-mtTA mice; 5B-582U (5′-gctccaggaaaccacaatgccttt-3′) and mtTA24L for Htr5B-mtTA mice; and GADup (5′-ACAGCGCATTAGAGCTGCTT-3′) and GADlow (5′-GCCAGCTTTCCCCTTCTAAA-3′) for GAD67-tTA mice. The sizes of the PCR products are approximately 230 bp, 300 bp, 680 bp, 630 bp, 380 bp, 600 bp, and 195 bp, respectively. Wild-type mice are negative for the above PCR products.

Immunohistochemistry

Mice were deeply anesthetized and perfused with 4% paraformaldehyde in 0.1 M phosphate buffer (PB). Brains were removed from the skull and post fixed overnight. After overnight cryoprotection with 20% sucrose/PB, brains were frozen, were cut at 25 μm thickness, and were mounted on silane-coated glass slides (Matsunami Glass, Tokyo, Japan).

Sections were rinsed with phosphate-buffered saline containing 0.1% Triton X-100 (PBST) 3 times, then treated with blocking solution (5% normal goat serum, 0.01% sodium azide in PBST) for 1 hr. Rabbit anti-GFP polyclonal antibody (Molecular Probes, Eugene, OR, 1:1000) was applied overnight at 4°C. After washing with PBST 3 times, specimens were treated with secondary anti-rabbit IgG antibodies conjugated to Alexa Fluor 488 (Molecular Probes, 1:2000). Images were obtained on an inverted light microscope (BZ-9000, Keyence, Osaka, Japan).

For double immunohistochemistry of EYFP and Iba1, a rat anti-GFP monoclonal antibody (1:500, line GF090R, nacalai tesque Inc, Kyoto, Japan) and a rabbit anti-Iba1 polyclonal antibody (1:500, WAKO, Osaka, Japan) were applied overnight at 4°C. After washing 3 times with PBST, specimens were treated with species-specific secondary antibodies conjugated to Alexa Fluor 488 or 568 (Molecular Probes, 1:2000). Images were obtained with a confocal microscope (LSM510, Carl Zeiss, Oberkochen, Germany).

In Situ Hybridization

The in situ hybridization method was described previously (Ma et al., 2006). In brief, digoxigenin-labeled *c-fos* cRNA probes (Pizoli et al., 2002) were hybridized to sections, NBT/BCIP compounds (Roche) were used for color development, and nuclear fast red (Vector Lab, Burlingame, CA, USA) was used for counterstaining.

For double fluorescence in situ hybridization, FITC-labeled *GLAST* cRNA probes (marker for astrocytes) and DIG-labeled *c-fos* cRNA probes were hybridized. After stringent washing, peroxidase-conjugated anti-DIG antibody (Roche, Indianapolis, IN, USA) was applied, and probes were visualized with Cy3 (TSA Plus Cyanine 3/Fluorescein System, Perkin Elmer, Foster City, CA, USA). After quenching peroxidase with hydrogen peroxide, peroxidase-conjugated anti-FITC antibody (Perkin Elmer) was applied and probes were visualized with FITC (TSA Plus TSA plus Cyanine 3/Fluorescein System).

Acute Brain Slice Preparations and Patch-Clamp Recordings

Brain slices were prepared from mice aged postnatal days 14–21. The animals were anesthetized by inhalation of halothane before decapitation, and the brain was sliced in ice-cold solution containing (in mM) 119.0 NaCl, 2.5 KCl, 0.1 $CaCl_2$, 3.2 $MgCl_2$, 1.0 NaH_2PO_4, 26.2 $NaHCO_3$, and 11.0 D-glucose (saturated with 95% O_2–5% CO_2). Slices were cut at a thickness of 250–400 μm using a microslicer (PRO7, Dosaka EM, Japan). The slices were then incubated in the above solution with $CaCl_2$ and $MgCl_2$ concentrations substituted to 2.0 mM and 1.3 mM, respectively, at 34°C for 30 min and then stored at room temperature. The slices were transferred to

a submerged-type recording chamber and continuously superfused. All recordings were performed at room temperature (22–25°C). Cells were visualized using a × 60 water immersion objective (0.9 numerical aperture) on a BX61WI upright microscope (Olympus, Japan) equipped with infrared-differential interference contrast. Whole-cell recordings were made with an Axopatch 200B patch-clamp amplifier and a Digidata 1440A digitizer controlled by pCLAMP 10 software (Molecular Devices, Union City, CA, USA). Patch electrodes with resistances of 3–4 MΩ were used. Cells were voltage clamped at –70 mV. The internal solutions contained (in mM): 142 K-gluconate, 2 KCl, 10 HEPES, 4 MgCl$_2$, 4 Na$_2$ATP, 0.5 NaGTP, and 0.05 EGTA (pH 7.2 with KOH titration). Signals were filtered at 2 kHz and digitized at 10 kHz. High power blue LED (470 nm; Luxeon V LXHL-PBO2, Lumileds Lighting; 8 mW at sample location) was placed underneath the condenser lens for full-field activation of ChR2(C128S) and yellow light, filtered (560 nm center 14 nm band-pass filter; FF01-560/14, Semrock; 0.15 mW at sample location) from a mercury lamp, was directed through the epifluorescence port for closing of the ChR2(C128S). 40 μM Alexa 594 was included in the patch pipette, and two-photon excitation was used to visualize cell morphologies (shown in magenta). Single-photon confocal images of EYFP expression in the targeted cells (shown in green) were overlaid.

In Vivo Electrophysiological Recording and Optical Stimulation of Hippocampal Neurons

To fix the head of the mouse in a stereotaxic apparatus, a small U-frame head holder was mounted on the head. Each mouse was anesthetized with ketamine hydrochloride (100 mg/kg body weight, i.p.) and xylazine hydrochloride (5 mg/kg body weight, i.p.) and fixed in a conventional stereotaxic apparatus. The skull was widely exposed, and periosteum and blood on the skull were removed completely. The exposed skull was completely covered with BISTITE II resin (Tokuyama, Tokyo, Japan) and UNIFAST II acrylic resin (GC corporation, Tokyo, Japan), and then a small U-frame head holder for head fixation was mounted and fixed with acrylic resin on the head of the mouse. After recovery from the first surgery (2 or 3 days later), the mouse was positioned in a stereotaxic apparatus with its head restrained using the U-frame head holder under light anesthesia with ketamine hydrochloride (50–100 mg/kg body weight, i.p.). A part of the skull in one hemisphere was removed to access the hippocampus.

After full recovery from the second surgery, the mouse was positioned in a stereotaxic apparatus with its head restrained using a U-frame head holder under anesthesia. For recording neural activity while illuminating with blue light, a glass-coated Elgiloy micro-electrode (0.5–1.0 MΩ at 1 kHz), along with a 50 μm diameter optical fiber (CeramOptec Industries, East Longmeadow, MA, USA), was inserted perpendicularly into the brain through the dura mater using a hydraulic microdrive (Narishige Scientific Instrument, Tokyo, Japan). A 50 mW blue laser (CrystaLaser, Reno, NV, USA) was coupled to an optical fiber. The laser was controlled via TTL pulses driven by a stimulator (Nihon Kohden, Tokyo, Japan). The target area was 2.0–3.0 mm posterior and 1.5–3.0 mm lateral to bregma and 1.2–1.6 mm deep from the brain surface for the hippocampus (Franklin and Paxinos, 2008). Signals from the electrode were amplified, filtered (0.3–10 kHz), and sampled at 50 kHz using a computer.

To extract ripple-like synchronous activity, the recorded data were band-pass filtered at 150–300 Hz. Ripple-like events were automatically detected based on their oscillatory powers and durations; the root mean square (3 ms window) of the band-passed signal was used to detect the ripple wave with a power threshold of 5 SDs with 10 ms in duration.

In Vivo Optical Stimulation of Freely Moving Mice

Violet light was generated by laser diode (445 nm, 400 mW, LDCU8/9164 Power Technology Inc., IL, USA) and applied through plastic optical fibers (ESUKA, Mitsubishi Rayon, Tokyo, Japan, 0.5 mm diameter). A pulse generator (SEN-8203 Nihon Kohden, Tokyo, Japan) controlled timing and power output of the laser diode. An optical swivel (COME2, Lucir, Tsukuba, Japan) was used for unrestricted in vivo illumination. Violet light power intensity at the tip of the plastic fiber was 6.7 mW/mm^2, measured by a power meter (VEGA, Ophir Optronics Ltd., Wilmington, MA, USA). For hippocampal CA1 pyramidal neuron stimulation, a plastic optical fiber was inserted above the left dorsal hippocampus using a stereotaxic frame (David Kopf Instruments, Tujunga, CA, USA) with the tip of the fiber located at 2.0 mm posterior, 1.5 mm lateral to bregma, and 1 mm deep from the skull. The fiber was fixed on the skull using dental cement. For astrocyte stimulation, the plastic fiber was placed on top of the skull (0.5 mm anterior and 1.5 mm lateral to bregma) and fixed with the dental cement. The mice were allowed to recover for at least 1 week after fiber implantation. For hippocampal neuron stimulation, 500 ms illumination was given every 1 min in the home cage, and locomotive activity was captured with a video camera (HDR XR550V, Sony, Tokyo, Japan) and analyzed with the aid of a Manual Tracking plug-in for FIJI software (distributed under the General Public License). For astrocyte stimulation, 500 ms illumination was given every 10 s in the home cage.

SUPPLEMENTAL REFERENCES

Baron, U., Gossen, M., and Bujard, H. (1997). Tetracycline-controlled transcription in eukaryotes: novel transactivators with graded transactivation potential. Nucleic Acids Res. *25*, 2723–2729.

Farley, F.W., Soriano, P., Steffen, L.S., and Dymecki, S.M. (2000). Widespread recombinase expression using FLPeR (flipper) mice. Genesis *28*, 106–110.

Franklin, K.B.J., and Paxinos, G. (2008). The mouse brain in stereotaxic coordinates, compact 3rd ed. (New York: Academic Press).

Hirasawa, T., Ohsawa, K., Imai, Y., Ondo, Y., Akazawa, C., Uchino, S., and Kohsaka, S. (2005). Visualization of microglia in living tissues using Iba1-EGFP transgenic mice. J. Neurosci. Res. *81*, 357–362.

Lakso, M., Sauer, B., Mosinger, B., Jr., Lee, E.J., Manning, R.W., Yu, S.H., Mulder, K.L., and Westphal, H. (1992). Targeted oncogene activation by site-specific recombination in transgenic mice. Proc. Natl. Acad. Sci. USA *89*, 6232–6236.

Ma, J., Matsumoto, M., Tanaka, K.F., Takebayashi, H., and Ikenaka, K. (2006). An animal model for late onset chronic demyelination disease caused by failed terminal differentiation of oligodendrocytes. Neuron Glia Biol. *2*, 81–91.

Matthes, H., Boschert, U., Amlaiky, N., Grailhe, R., Plassat, J.L., Muscatelli, F., Mattei, M.G., and Hen, R. (1993). Mouse 5-hydroxytryptamine5A and 5-hydroxytryptamine5B receptors define a new family of serotonin receptors: cloning, functional expression, and chromosomal localization. Mol. Pharmacol. *43*, 313–319.

Nakayama, M., and Ohara, O. (2005). Improvement of recombination efficiency by mutation of red proteins. Biotechniques *38*, 917–924.

Pizoli, C.E., Jinnah, H.A., Billingsley, M.L., and Hess, E.J. (2002). Abnormal cerebellar signaling induces dystonia in mice. J. Neurosci. *22*, 7825–7833.
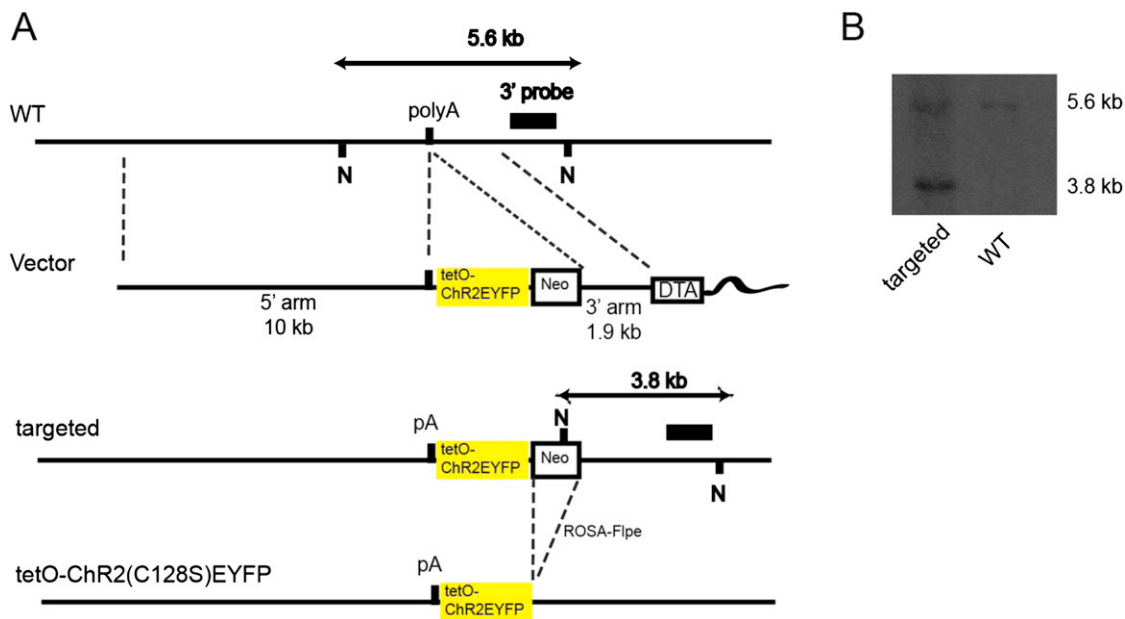
Figure S1. tetO-ChR2(C128S)-EYFP Knockin, Related to Figure 1

(A) Schematic diagram indicating the targeting vector comprised of 10 kb 5′ homology arm, tetO-ChR2(C128S)-EYFP pA-Neo cassette, 1.9 kb 3′ homology arm, and DTA. Neo cassette flanked by FRT sites was removed by crossing with ROSA-Flpe mice.

(B) Targeted embryonic stem (ES) clone was screened by Southern blotting with 400bp 3 prime outside probe, which identified a 5.6 kb fragment of wild-type allele and a 3.8 kb fragment of the targeted allele in genomic DNA.
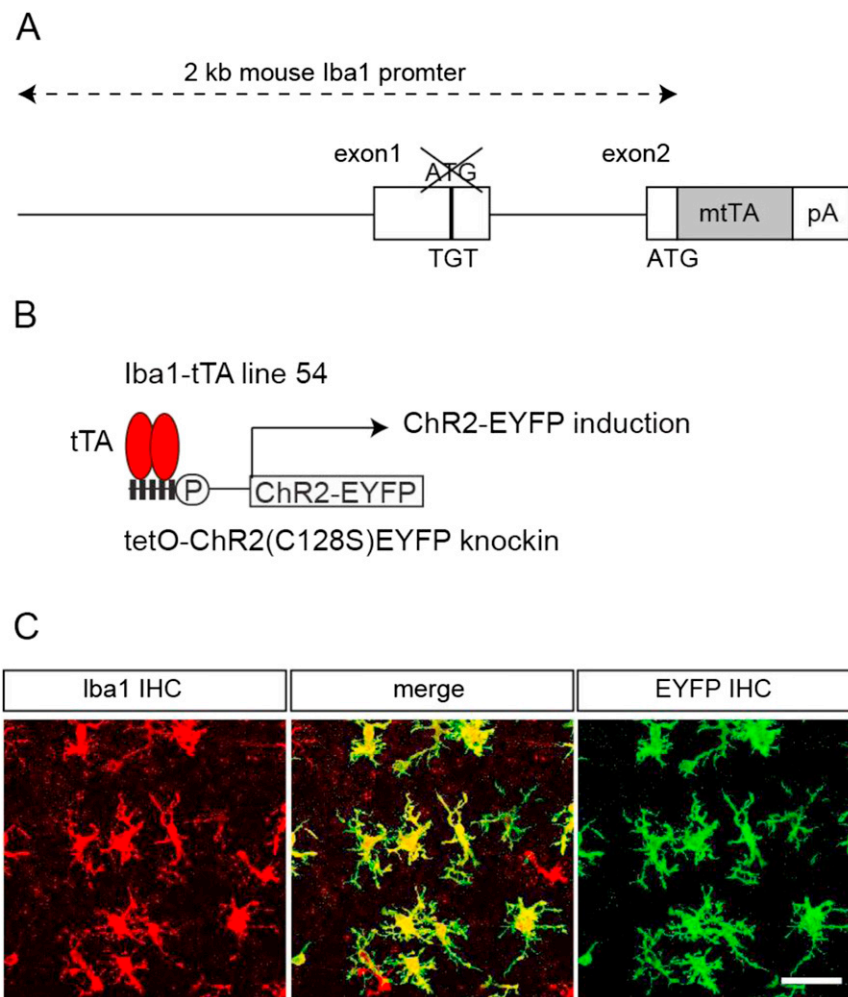
Figure S2. Iba1 tTA Mouse, Related to Figures 2 and 3

(A) DNA alignment of Iba1 tTA transgene.

Modified Iba1 promoter consists of an 1.6 kb 5′ flanking DNA, exon 1, intron 1, and 12 bp of exon 2 of the mouse Iba1 gene. The original translation initiation site (ATG) in exon 1 was replaced with TGT so that translation started from the ATG of the mtTA cDNA in exon 2. An SV40 polyadenylation signal (polyA) was used.

(B) tTA-mediated gene induction.

mtTA protein was expressed under the control of the Iba1 promoter. tTA binds to the tTA-dependent promoter (tetO) and transactivates the transcription of ChR2(C128S)-EYFP in Iba1 expressing cells in Iba1-tTA line 54::tetO-ChR2(C128S)-EYFP knockin double transgenic mice.

(C) tTA-mediated gene induction in Iba1 positive cells.

Double-immunohistochemistry of Iba1 and EYFP showed that Iba1 positive cells (red), in this case microglia, expressed EYFP (green). Within the hippocampus at postnatal days 21, 68% of Iba1 positive cells expressed EYFP in Iba1-tTA line 54::tetO-ChR2(C128S)-EYFP knockin double transgenic mice. Scale: 50 μm.
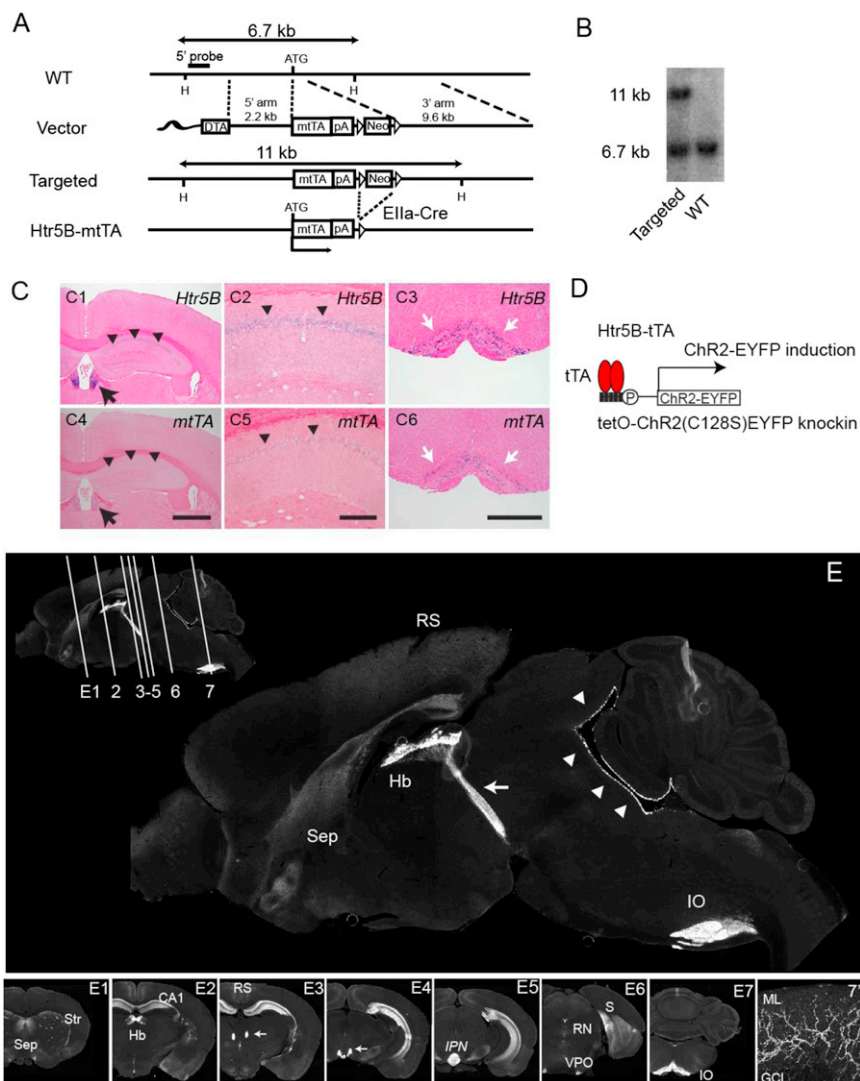
Figure S3. Htr5B-tTA Knockin Mouse, Related to Figure 3

(A) Schematic diagram indicating the targeting vector comprised of DTA, 2,2 kb 5′ homology arm, mtTA-polyA-Neo cassette and 9.6 kb 3′ homology arm.

(B) Targeted embryonic stem (ES) clone was screened by Southern blotting with 400bp 5 prime outside probe, which identified a 6.7 kb fragment of wild-type allele and an 11 kb fragment of the targeted allele in genomic DNA.

(C) In situ hybridization of Htr5B and mtTA mRNA in Htr5B-tTA mice. Both Htr5B and mtTA mRNAs were strongly expressed in the medial habenula (black arrow in C1,C4) and inferior olive (white arrows in C3,C6), moderately expressed in hippocampal CA1 region (arrowheads in C2,C5). This expression profile was consistent to previous reports (Matthes et al., 1993) and data from GENSAT (image 27454 and 27455). Scales: 1 mm in C1,3,4,6; 200 μm in C2,5.

(D) tTA-mediated gene induction in Htr5B expressing cells.

(E) tTA-mediated ChR2(C128S)-EYFP induction in Htr5B-tTA::tetO-ChR2(C128S)-EYFP knockin bigenic mice. ChR2(C128S)-EYFP was labeld by immuno-staining of EYFP. Sagittal section showed strong EYFP expression in the medial habenula (Hb) and the inferior olive (IO). Diagram in the upper-left corner shows the levels of coronal sections. Axons of medial habenula neurons, termed fasciculus retroflexus, were labeled by EYFP (arrows in E, E3, E4) and they terminated at intrapeduncular nucleus (IPN in E5). Axons of inferior olive neurons, termed climbing fibers, were visualized in the cerebellar lobes (7′, ML: molecular layer; GCL: granule cell layer in the cerebellum). CA1 pyramidal neurons strongly expressed EYFP (E2-E5). Retrosplenial cortex (RS), striatum (Str), septum (Sep), raphe nucleus (RN), subiculum (S), ventral periolivary nucleus (VPO) showed weak EGFP expression. In addition to neuronal cells, Ependymal cell expressed EYFP (arrows in E).
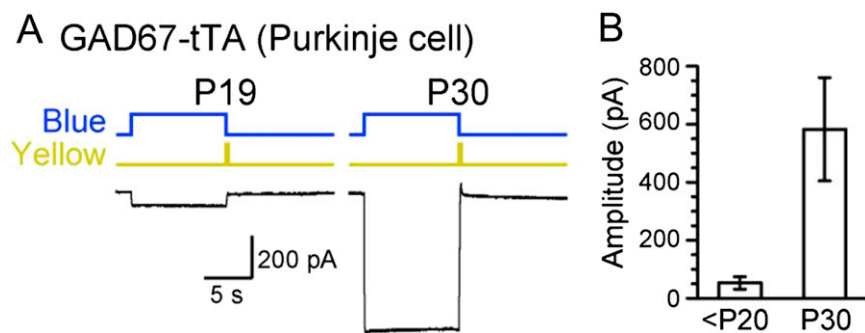
Figure S4. Age Dependence of Photocurrent, Related to Figures 3 and 4

(A) Representative ChR2(C128S) photocurrents recorded from Purkinje cells in P19 and P30 mice (GAD67-tTA::tetO-ChR2(C128S)) in the presence of TTX, Cd^{2+}, PIC, and NBQX.

(B) Summary of the amplitudes of the photocurrent (<P20, n = 6; P30, n = 3 cells). Error bars: SEM.